A Valence Bond Study of the Bonding in First Row Transition Metal Hydride Cations: What Energetic Role Does Covalency Play?

ARTICLE *in* THE JOURNAL OF PHYSICAL CHEMISTRY · FEBRUARY 2000

Impact Factor: 2.78 · DOI: 10.1021/jp9924878

3 AUTHORS:

John Morrison Galbraith
Marist College
32 PUBLICATIONS **590** CITATIONS
SEE PROFILE

A. Shurki
Hebrew University of Jerusalem
49 PUBLICATIONS **1,308** CITATIONS
SEE PROFILE

Sason Shaik
Hebrew University of Jerusalem
527 PUBLICATIONS **20,677** CITATIONS
SEE PROFILE

A Valence Bond Study of the Bonding in First Row Transition Metal Hydride Cations: What Energetic Role Does Covalency Play?†

John Morrison Galbraith,‡ Avital Shurki, and Sason Shaik*

Department of Organic Chemistry and the Lise Meitner-Minerva Center for Computational Quantum Chemistry, The Hebrew University, Jerusalem 91904, Israel

Received: July 20, 1999; In Final Form: November 8, 1999

The transition metal hydride cations, TMH^+ (TM = first transition metal row, Sc, Ti, V, Cr, Mn, Co, Ni, Cu, and Zn), have been studied using valence bond (VB) theory to elucidate the bonding in these systems through VB concepts. Although the bonds appear extremely covalent by virtue of charge distribution, this appearance conceals key contributions to bonding, such as covalent-ionic resonance energy (RE_{CS}) and relaxation energy of the inactive electrons (ΔE_{relax}(inactive)). The RE_{CS} term is seen to increase from ScH^+ toward ZnH^+, becoming significant in the late TMH^+ molecules. The ΔE_{relax}(inactive) term, which accounts for the nonbonding $3d^n$ electrons and the $3s^23p^6$ core electrons, is always significant. Furthermore, for all of the bonds from CrH^+ to CuH^+, the relaxation term makes a major contribution to the bond energy. It appears therefore, that in these TM−H^+ bonds, the spin pairing of the bonding electrons can act as a trigger for the nonbonding and adjacent core electrons to relax their Pauli repulsion and thereby strengthen the binding of TM^+ and H. As a result of the general weakness of TM bonds, the relaxation is expected to frequently be an important bonding contribution. The major function of the inactive and core electrons shows that the traditional role of "covalency" must be reassessed in a systematic manner.

I. Introduction

Transition metal complexes play an important role in the areas of surface and homogeneous catalysis,[1] metallo-enzymatic biochemistry[2], and astrophysics.[3] This wide range of applications has stimulated intense research activity focused on properties of transition metal complexes.[3−32] Many of these studies have been devoted to small molecules, such as transition metal hydride cations, transition metal oxo cations, etc., in the hope that the insight can be extrapolated to larger, more complicated systems. Indeed, understanding the bonding between transition metal and main elements remains a challenging field for theoretical chemistry, with intellectual and practical implications.

Previous theoretical studies of TMH^+ molecules[10−14,38] showed that accurate prediction of bond dissociation energies (BDEs) requires extended wave functions that involve treatment of both static and dynamic electron correlation. A few extensive studies have been carried out by Goddard et al.[10−13] using the GVB-DCCI method, which involves a generalized valence bond (GVB)[38] calculation augmented by dissociation consistent CI, and by Bauschlicher et al.,[14] who used correlated molecular orbital (MO) methods such as the modified coupled pair functional method (MCPF) and CASSCF augmented by CISD, etc. More recently, Ziegler and Li[15] have determined the contribution to the BDEs of TMH^+ due to various components of density functional theory, and Barone and Adamo[16] have employed hybrid Hartree−Fock/density functional methods to test the accuracy of such methods for use with transition metal complexes.

The studies of Goddard et al.[10−13] and Bauschlischer et al.[14] highlighted the importance and difficulties of a balanced correlation treatment of the $4s^13d^n$ and $3d^{n+1}$ states of the metal cation. Their GVB study[11] showed that the GVB wave function by itself is unable to provide quantitative accuracy and that additional extensive CI is needed to achieve this accuracy. Nevertheless, the GVB treatment predicts correct trends that clarify the bonding patterns in first row TMH^+ in terms of a few concepts[10] such as the metal cation promotion energy associated with excitation from the $3d^{n+1}$ state to the bond-forming $4s^13d^n$ state, the loss of exchange in the $4s^13d^n$ state following spin pairing of the 4s electron with the hydrogen atom, and the choice of the ground state symmetry determined by the electrostatic repulsion between the d electrons. It is apparent therefore that VB theory is capable of providing very useful insight into bonding because it involves a compact, easily interpretable wave function. A complement to the GVB studies[10−13] can come from classical VB theory, which uses explicit covalent and ionic structures and in its current implementation[33−37] can provide bonding patterns in terms of covalency, covalent-ionic resonance energy, and relaxation of the bonding, the 3d and the $3s^23p^6$ shell electrons.

SCHEME 1

The appeal of classical VB theory stems from the close association with the fundamental concept of the electron pair bond originally developed by Lewis[39] and Langmuir[40] and further couched in quantum chemical language by Pauling.[41] From this perspective, an electron-pair bond is generated from the three principal structures in Scheme 1: A•−• B (**1a**), which is the covalent Heitler−London (HL)[42] form that owes its bonding to electron spin pairing, and the ionic types A^+ **:**B^- and A^- **:**B^+ (**1b,c**), which can mix with the covalent structure

† Dedicated to the memory of Professor J. Gerratt.

‡ Present address: Department of Chemistry, Box 351700, University of Washington, Seattle, WA 98195-1700.

10.1021/jp9924878 CCC: $19.00
Published on Web 01/22/2000

to extents depending on properties of the atom such as ionization potentials, electron affinities, etc. This kind of information is latent in the GVB wave function, which itself is a mixture of these structures[43] as a result of the delocalization tails of the pseudoatomic orbitals (Coulson−Fischer AOs[44]).

The breathing orbital VB (BOVB) method, from Hiberty et al.,[34−37,45,46] retains the classical three-configuration nature of the bond wave function and at the same time retrieves part of the dynamic correlation, the part that is associated with the response of the "inactive" electrons to the bonding event. As such, the classical VB method in its modern form enables derivation of new insight into the nature of the chemical bond.[47−51] One such new feature is the recently described charge-shift (CS) bonding,[47−50] in which the bonding is due neither to spin pairing of the covalent form nor to the ionicity inherent in the ionic forms, but rather to the resonance interaction of the forms.[47,49] Even homonuclear bonds such as F−F, O−O, N−N, etc, are CS bonds. Another such feature is the relaxation of the inactive electrons in response to the bond-pairing, an effect which has been shown significant in some bonds of main elements.[49] Accordingly, the present paper begins to explore the importance of these effects in transition metal bonding and as a first step in TM−H^+ bonds.

II. Methods

Three different basis sets were tried: one is an all-electron basis set, and the other two involve basis functions for the 3s, 3p, 3d, and 4s orbitals and a relativistic effective core potential (RECP) for the $1s^22s^22p^6$ core. Starting with the RECPs, the first basis set, designated as Hay−Wadt (HW), is based on the RECP of Hay and Wadt[52] on the metal atom and consists of a double ζ (5s,5p,5d//3s,2p,2d) basis on the metal in conjunction with the double ζ (4s//2s) basis of Dunning on H[53] augmented with a p-type polarization function ($\alpha_p = 0.10$). The second, designated ST, is based on the RECP developed in the Stuttgart group by Dolg et al.[54] and involves a triple ζ (8s,7p,6d//6s,-5p,3d) basis on the metal in conjunction with the triple ζ (5s//3s) basis of Dunning[55] on H augmented with a p-type polarization function ($\alpha_p = 0.75$). The all-electron basis set, designated as Wachters, consists of Wachters's basis functions[56] on the metal atom (14s,11p,6d//8s,6p,4d) with Dunning's triple ζ basis on H as described above. In addition, f-type functions were added[57] to the metal atoms, and the resulting basis sets are designated +f, for example, ST+f.[58] In all calculations involving the Wachters basis set the 1s, 2s, and 2p metal orbitals were kept frozen.

An initial test of the ECPs and basis set used ScH^+ and CrH^+. The HW and HW+f combinations were judged less appropriate by these tests. The test further showed that the ST or ST+f combinations give bond BDEs in agreement with the all-electron basis set and close to experimental values. The f-orbitals were found to ensure orbital convergence to the global minimum. Their removal had little effect on the BDE values.

The ground-state configurations of all TMH^+ species followed the Ohanessian−Goddard[10] assignment. As a gauge for the VB calculations we use the coupled cluster method, which includes single and double excitations with the perturbative addition of triple excitations [CCSD(T)].[59,60] All CCSD(T) calculations were carried out with the GAUSSIAN94 suite of programs.[61]

The VBSCF and BOVB Methods. The VB calculations were carried out using the Utrecht package TURTLE,[33a] which is a general nonorthogonal CI program that simultaneously optimizes the VB coefficients (c_1−c_3, eq 1 below) and the orbitals. This optimization procedure is based on the super-CI technique,[62,63] which is related to the generalized Brillouin theorem.[64] By use of the three VB structures, the active (bonding) electrons are correlated while the inactive (nonbonding) electrons are described by a set of singly and doubly occupied orbitals that adjust to the fluctuating density of the bond pair.

SCHEME 2

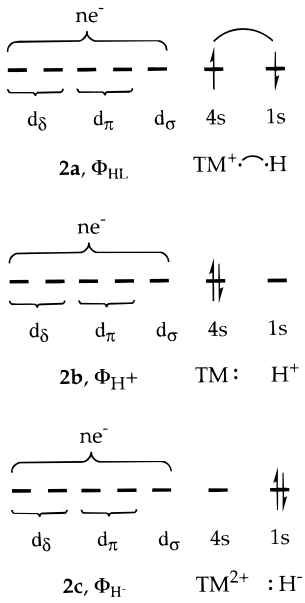

The two-electron bonds in the TMH^+ species can most simply be described by the fundamental configurations in Scheme 2; the covalent Heitler−London (HL) structure, $TM^+\bullet-\bullet H$ (**2a**), hereafter referred to as Φ_{HL}, and "ionic" structures, TM**:** H^+ (**2b**) and TM^{2+}**:**H^- (**2c**), designated Φ_{H^+} and Φ_{H^-}, respectively. It can be seen from **2a** that the Φ_{HL} structure involves a covalent bond that utilizes the 4s orbital of the metal, in the $4s^13d^n$ configuration. However, because the d_σ orbital ($3d_{z^2}$) has the same symmetry as 4s, there will be some hybridization that will be taken care of automatically through the orbital optimization procedure. It is also important to note that the protio and hydrido structures are related to Φ_{HL} by electron transfer to and from the 4s orbital (hybridized to some extent with the d_σ). Additional configurations that were added to the structure set proved unnecessary (e.g., using separate HL configurations for TM^+-4s-H1s and TM^+3d_σ-H1s bonding). The ground state of the Cu^+ cation has a completely filled d-shell, and therefore the $3d^{10}$ VB configuration and its corresponding ionic structures were included in the VB structure set for CuH^+. This however did not change the BDE sufficiently to merit special account. Thus, the three VB structures (Scheme 2) and the orbital optimization correspond to a stable model wave function.

Within the minimal VB structure set in Scheme 2, the bond wave function becomes

$$\Psi_{TMH^+} = c_1\Phi_{HL} + c_2\Phi_{H^+} + c_3\Phi_{H^-} \qquad (1)$$

At the lowest VB level, designated VBSCF,[33b] there is a common set of orbitals for both ionic and HL structures that are strictly localized on each fragment, TM or H. Thus, at the VBSCF level, the orbitals and structural coefficients respond to an average field of the VB structures. The VBSCF description of the electron pair is equivalent[43] to the more compact descriptions by the GVB[38] and SCVB[65,66] theories, which use a single VB structure with atomic orbitals that possess delocalization tails.[44]

An alternative is to remove the average field restriction and allow a unique set of orbitals for each VB structure. In this manner, each orbital can fluctuate dynamically in size and shape and adjust to the local charge of the VB structure, as well as to the mixing with the other structures. This method,[34−37] the so-called breathing orbital valence bond (BOVB), brings in some dynamic correlation and is therefore more accurate than VBSCF while conserving the same compact wave function.

Allowing the inactive electrons to delocalize over both fragments while keeping the active electrons localized has been shown to be advantageous in certain cases.[34] However, in the present situation, this procedure was tested and found to be unnecessary. Therefore all electrons are held strictly localized and the resulting BOVB wave function carries the designation L-BOVB. All of the VB methods were tested initially on ScH^+ ($^2\Delta$) and CrH^+ ($^5\Sigma^+$) and compared with CCSD(T) results. These tests singled out L-BOVB/ST+f as a sufficiently accurate level for the series.

Atomic States at the Dissociation Limit. With the minimal VB structure set, the VB wave function correlates with restricted open-shell Hartree−Fock (ROHF) states of the TM^+ and H. Because the HF level treats poorly the atomic states and especially the $3d^{n+1}$ state, the deficiencies in the atomic calculation will carry over to the BDE values, even if the molecular calculation is correct. Goddard et al.[10−13] and Bauschlicher et al.[14,67] showed that the deficiencies can be avoided by correcting the energies of the TM^+ fragment using experimental atomic data. Thus, the TMH^+ species are dissociated into the atomic electronic states most closely resembling their situation in the molecule (i.e., for TM^+ it is the $4s^13d^n$ state), and whenever necessary, the experimental atomic state splitting is used to correct the energy of the TM^+ fragment to the corresponding atomic ground state. This procedure has been adopted in the present case for V^+, Cr^+, Co^+, Ni^+, and Cu^+. In the cases of Cr^+ and V^+, the $3d^{n+1}$ and $4s^13d^n$ configurations are of the same spatial and spin symmetry, and therefore the molecule smoothly dissociates to the $3d^{n+1}$ atomic ground state. For Cr^+ the HF energy of the $3d^{n+1}$ configuration is overestimated relative to the $4s^13d^n$ configuration, the resulting BDE is too high. Dissociation to the $4s^13d^n$ configuration and application of the Goddard−Bauschlicher corrective procedure improve the BDE value. For V^+ the ground state at the HF level is erroneously calculated to be $4s^13d^n$ and the correction due to experimental splitting must be applied. All values for atomic splitting are taken from Moore.[68]

Inclusion of All Rumer Diagrams. For a given number of electrons there exist a few linearly independent spin coupling schemes nascent from a given configuration and possessing the same total spin quantum number.[69] To account for these coupling schemes, we use Rumer diagrams[69] for the covalent structure, e.g., for ScH^+ in Scheme 3 there exist two such Rumer schemes: **3a** pairs the TM 4s and H 1s electrons[70] and **3b** pairs the TM d_δ and H 1s electrons. Of course, only the former scheme is a proper HL structure that leads to bonding, whereas the latter is expected to have a small effect on the total energy. As the number of unpaired d electrons increases, so will the number of Rumer schemes.[69]

The energetic effect of the nonbonded Rumer schemes was tested and found to be small, never exceeding 2.8 kcal mol^{-1} at the VBSCF/ST+f level, as depicted in Figure 1. Because the BOVB wave function has difficulty converging with an increasing number of Rumer structures, it was decided to wave the small effect of the full Rumer set at this level. Accordingly, at the VBSCF level, both BDE and geometry were determined

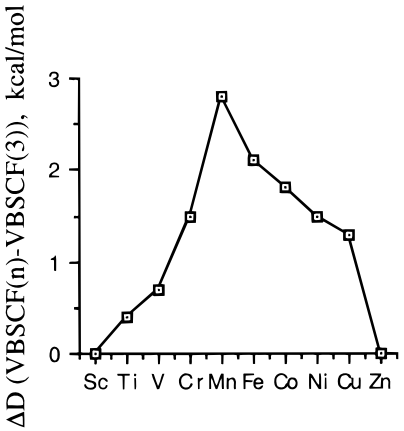

Figure 1. The VBSCF TMH^+ energetic stabilization upon inclusion of all Rumer structures. The stabilization peaks for MnH^+ with the maximum possible spin pairings. Stabilization is higher for the heavier transition metal hydride cations as a result of more favorable spin pairing with the singly occupied d_σ.

SCHEME 3

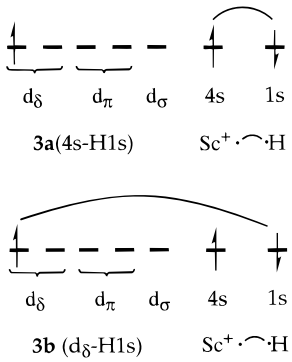

with all structures, whereas at the BOVB level only the dominant HL bond-pair structure and the corresponding ionic structures in eq 1 were used. The effect of including all Rumer structures as determined at the VBSCF level can then be added to the three-configuration BOVB as a correction. Consequently, the BOVB wave function is generally a three-structure situation as in eq 1. All qualitative bonding analyses for both VBSCF and BOVB use only the dominant bond-pair and corresponding ionic structures. To specify the level, the number of VB structures is indicated in parentheses, e.g., VBSCF(n) or BOVB(n) refer to the n-fold-structure wave function, and when $n = 3$ the wave function in eq 1 is invoked.

Comments on the Use of BOVB. The breathing orbital effect brings in dynamic correlation by accounting for the instantaneous response of the active and inactive orbitals to the charge fluctuation inherent in the three VB structures of Scheme 2. In technical terms, this orbital relaxation effect is akin to orbital optimization through single excitations.[34−37,64] Let us imagine, however, a case where the BOVB procedure leads to inactive orbitals that are very different in the HL and ionic configurations (e.g., an inactive pair in an ionic structure occupies an orbital that is mostly virtual in the HL structure). In such a case, the VB mixing starts resembling the mixing of configurations that differ by double excitations, like in a CID (configuration interaction doubles) treatment. This would bring in an *additional* correlation effect that stabilizes only the molecule but not the fragments, because at the separate fragment asymptote the HL structure is the only VB configuration that remains while the ionic contribution to the wave function drops to zero. Consequently, the fragments would not enjoy this additional correla-

tion, and some overbinding will result. This has been noted in our study for ZnH^+.

The way to correct this overbinding due to double excitation is to use a wave function where all the inactive pairs are equally correlated at the molecular and atomic limits by splitting the inactive filled orbitals.[46,49,71,72] This, however, renders the BOVB procedure too cumbersome, if not technically impossible, to use. An effective corrective procedure uses a redundant structure, Φ_{HL}' that has identical bond orbitals with the bond-paired Φ_{HL} structure, but which is allowed to have differently optimized inactive orbitals. The calculations are performed both at the molecular geometry and at a separated fragments' asymptote (calculated at 10 Å). Because at the dissociation asymptote both Φ_{HL} and Φ_{HL}' are present, any excess stabilization of the inactive orbitals in the molecule can be counterbalanced by a similar effect in the separated fragments. In the case of ZnH^+, using this redundant structure technique at the equilibrium geometry and at 10 Å deleted the overbinding effect. For the other TMH^+ species no overbinding was apparent, and the corrective procedure, when successful, yielded small changes (3 ± 1 kcal mol^{-1}) and hence as a result of technical difficulties was not used routinely.

Methods for Analyzing the VB Wave Functions. The weights of VB states were determined by the formula of Coulson−Chirgwin[73] (eq 2) , which is the VB analogue of the

$$w_i = c_i^2 + \Sigma_j c_i c_j S_{ij} \quad (2)$$

Mulliken population analysis.

Perturbation theory formalism with retention of overlap between the VB structures[74,75] was used to analyze the VB mixing. Thus, much like in the corresponding MO mixing,[76] in the VB mixing too the effective matrix element that determines the mixing strength of a given high-lying structure (Φ_i) into the lowest structure (Φ_0) is the reduced matrix element given by[74,75] eq 3 where H_{0i} is the direct matrix element of the HL

$$\beta_i = H_{0i} - e_0 S_{0i} \quad (3)$$

and ionic configurations, Scheme 2, S_{0i} is the overlap, and e_0 is the energy of the lowest VB structure (the HL configuration). The corresponding mixing coefficient, λ, is given in eq 4, and the energy stabilization due to this mixing is given in eq 5.

$$\lambda_i = \beta_i/(e_0 - e_i) \quad (4)$$

$$\Delta E_i = \lambda_i \beta_i \quad (5)$$

Determination of the Various Contributions to the Bond Energy. Restricting the breathing orbital effect to selected groups of electrons allows the assignment of the orbital relaxation effect in a systematic manner as increments between differential computational levels (see Scheme 5). The orbital optimization/relaxation window is specified in the parentheses, following the number of VB structures, i.e., VBSCF(*n*,*m*) or BOVB(*n*,*m*), where *n* is the total number of configurations and *m* signifies the number of optimized electron pairs (e.g., *m* = full means that all active and inactive electrons are optimized, *m* = bp means that only the bond pair is optimized, and so on.)

To quantify the orbital relaxation effects, initially all of the orbitals are optimized at the VBSCF(3,full) level. The relaxation of the bonding electrons can be determined then as the energy difference between the VBSCF(3,full) and the BOVB(3,bp), where only the bond-pair electrons are allowed to breathe while all the others remain at their VBSCF optimized forms. A subsequent BOVB(3,bp+d) calculation also allows, in addition to the bond orbitals, the breathing of the valence 3d orbitals. The difference between this and the previous BOVB(3,bp) datum provides the relaxation effect of the valence nonbonding d electrons. Finally, BOVB(3,full) allows all of the orbitals to relax, and the difference relative to BOVB(3,bp+d) gives the relaxation energy of the core orbitals, which in the present case refer to the $3s^23p^6$ shell.

TABLE 1: TMH^+ Bond Lengths (Å) for the TM Series Sc to Zn

entry		VBSCF[a]	CCSD(T)	GVB[b]
1	ScH^+	1.861	1.796	1.810
2	TiH^+	1.789	1.704	1.730
3	VH^+	1.736	1.637	1.662
4	CrH^+	1.674	1.590	1.602
5	MnH^+	1.726	1.622	1.702
6	FeH^+	1.681	1.575	1.653
7	CoH^+	1.631	1.505	1.606
8	NiH^+	1.590	1.467	1.561
9	CuH^+	1.551	1.480	1.513
10	ZnH^+	1.575	1.511	1.545

[a] All values obtained at the VBSCF(*n*,full)/ST+f level where $n = 2S + 1$. [b] GVB-DCCI from ref 10.

III. Results

VB Results for the TMH^+ Series. The VBSCF(*n*,full) optimized bond lengths are listed in Table 1 along with the CCSD(T) bond lengths determined in this work and previous GVB(DCCI) results.[10] There are no experimental bond lengths for comparison. The VBSCF(*n*,full) bond lengths are seen to be, on average, 0.09 Å longer than the CCSD(T) predictions and only 0.04 Å longer than the GVB(DCCI) results. If one assumes the CCSD(T) bond lengths to be accurate, then the performance of the present VBSCF method is in accord with recent results in our lab[49] in which VBSCF overestimates experimental M−Cl (M = C, Si, Ge, Sn, Pb) bond lengths by 0.1 Å. Despite this quantitative difference, the VBSCF trends are the same as in the benchmark CCSD(T) results, where the TM−H^+ bond length shrinks as atomic number increases. The local jump in bond length at MnH^+ is due to repulsion between the bond and d_σ electrons and appears in all of the methods in Table 1.

Table 2 contains BDEs calculated at the VBSCF(*n*,full)/ST+f and L-BOVB(3,full)/ST+f levels, which are compared with the benchmark CCSD(T) values and with previous[11,14] computational results. The VBSCF results are seen to be somewhat better than the GVB[11] results. However, the VBSCF results are still low in comparison with experiment, the benchmark CCSD(T) data, and the other higher level calculations in Table 2.

Although too low, the VBSCF results do reproduce the experimental trends in BDE across the first TM row, as shown in Figure 2, which compares VBSCF(*n*,full), CCSD(T), L-BOVB-(3,full), and experimental values. The zigzag pattern along the series has been explained in a beautifully lucid manner by Ohanessian and Goddard[10] as being due to the variation of two effects: the atomic promotion energy to the $4s^13d^n$ state and the loss of 4s−3d exchange due to the pairing of the 4s electron into a bond. The added flexibility of the L-BOVB(3,full) method is seen to bring the predicted BDEs closer to CCSD(T), GVB-DCCI, MCPF, and experimental results (Table 2). Thus, the VBSCF and also GVB and SCVB methods capture the essential static correlation effects due to the bonding event, whereas L-BOVB, rather than changing this qualitative picture, adds the dynamic relaxation energy of all the electrons in response to bond pairing.

TABLE 2: Bond Dissociation Energies (kcal mol^{-1}) of TMH$^+$ Species[a]

entry		VBSCF(*n*,full)[b]	L-BOVB(3,full)[c]	CCSD(T)	GVB[c]	GVB-DCCI[d]	MCPF[e]	experimental[f]
1	ScH^+	46.4	57.5	55.2	47.4	57.5	56.0	57 ± 2
2	TiH^+	44.2	54.3	54.6	43.4	56.4	53.3	54 ± 3
3	VH^+	41.6	53.1	48.0	33.8	46.1	48.6	48 ± 2
4	CrH^+	9.5	26.1	37.3	8.9	26.9	27.7	32 ± 2
5	MnH^+	30.6	44.0	44.2	25.9	41.8	43.7	48 ± 3
6	FeH^+	36.0	53.9	51.9	31.2	49.4	52.3	50 ± 2
7	CoH^+	27.2	48.8	39.5	21.3	45.9	44.5	47 ± 2
8	NiH^+	16.1	40.3	39.3	9.7	38.2	41.0	40 ± 2
9	CuH^+	−16.3	11.4	24.4	−22.2	23.5	18.5	22 ± 3
10	ZnH^+	46.2	55.7[g]	56.0	46.5	55.1		55 ± 3

[a] All values obtained with ST+f basis. [b] Here, (*n*,full) means all *n*-Rumer structures are used, and all electron-pairs are optimized. [c] The Rumer corection is included in the BOVB datum. [d] Reference 11. [e] Reference 14. [f] Reference 19. [g] L-BOVB result for ZnH^+ utilized an additional covalent VB state as described in the text.

TABLE 3: TMH$^+$ Valence Bond Weights[a]**/Mixing Coefficients**[b]

		M$^+$•−•H		M^{2+}:H$^-$		M: H$^+$	
entry		VBSCF	BOVB	VBSCF	BOVB	VBSCF	BOVB
1	ScH^+	0.792/0.813	0.989/0.999	0.074/0.097	−0.059/−0.122	0.116/0.147	0.072/0.108
2	TiH^+	0.761/0.808	0.968/0.977	0.079/0.102	−0.048/−0.104	0.116/0.150	0.080/0.121
3	VH^+	0.737/0.808	0.976/0.987	0.067/0.087	−0.067/−0.119	0.127/0.165	0.091/0.131
4	CrH^+	0.699/0.808	0.995/1.008	0.073/0.089	−0.082/−0.142	0.116/0.164	0.087/0.129
5	MnH^+	0.639/0.817	0.961/0.972	0.058/0.073	−0.060/−0.108	0.120/0.182	0.098/0.145
6	FeH^+	0.670/0.810	0.977/0.990	0.053/0.066	−0.075/−0.131	0.135/0.192	0.098/0.146
7	CoH^+	0.686/0.806	0.978/0.993	0.045/0.056	−0.083/−0.143	0.149/0.206	0.105/0.155
8	NiH^+	0.754/0.802	0.985/1.00	0.040/0.050	−0.093/−0.156	0.168/0.215	0.107/0.157
9	CuH^+	0.723/0.793	0.993/1.017	0.039/0.047	−0.113/−0.189	0.168/0.225	0.120/0.179

[a] VB weights determined as in eq 2. [b] The corrective addition of Φ_{HL}' renders the weights and coeficients of ZnH^+ meaningless.

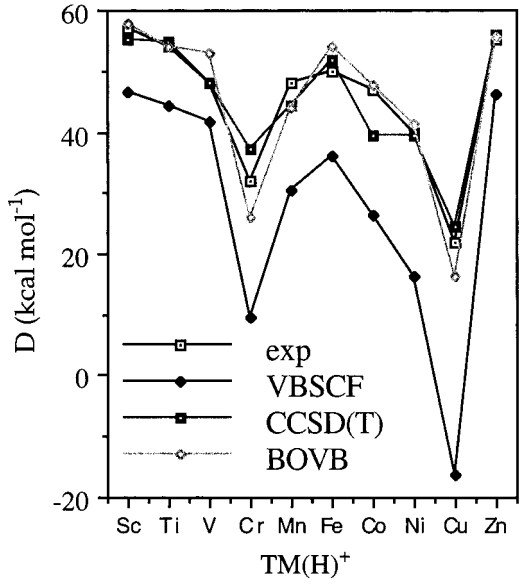

Figure 2. The experimental (from ref 19), VBSCF(*n*,full), CCSD(T), and L-BOVB(3,full) bond dissociation energies (*D*) in kcal mol^{-1}.

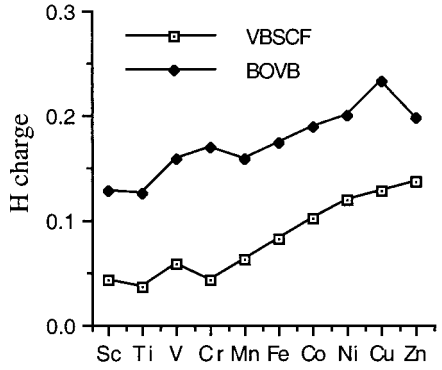

Figure 3. The amount of VBSCF(*n*,full) and L-BOVB(3,full) charge transfer from H to TM for the TMH$^+$ series.

VB Coefficients and Weights. Table 3 shows the VB mixing weights and coefficients at the VBSCF(3,full)/ST+f and L-BOVB(3,full)/ST+f levels. First, it is apparent that the TM−H$^+$ bonds are all predominantly covalent, at both levels, and the present results support the conclusion of Ohanessian and Goddard[10] that the oxidation state formalism is not supported for these bonds. In accord with the coefficients and weights of the ionic structures, the charge distribution in all the TM−H$^+$ bonds places a small positive charge on the hydrogen, as shown graphically in Figure 3. The uniform protio charge character is opposite to the uniform hydrido charge character in the GVB results[10,11] but in general agreement with the MCPF data, which show a protio charge from CrH^+ onward.[14] Nevertheless, in agreement with GVB and MCPF, the VBSCF or BOVB charges increase generally along the series. The charge increase is in general accord with the increase of the mixing coefficient and weight of the Φ_{H^+} structure. These trends are expected from the changes in the ionization energy and effective nuclear charge of the metal along the TM series.

A second point in Table 3, is that the hydrido structure (Φ_{H^-}) is significantly less important than the protio structure (Φ_{H^+}), again in contrast with the oxidation state formalism. A better perspective of the relative importance of the two configurations will be obtained later by analyzing the energy contribution due to the VB mixing.

Finally, another feature in Table 3 is the change in sign of the mixing coefficient of the Φ_{H^-} structure from positive in VBSCF to negative in L-BOVB.[49] The negative Φ_{H^-} coefficient accounts for the corresponding negative weight, which originates in the overlap population terms in the Coulson−Chirgwin formula, eq 2, and especially the term between Φ_{H^-} and the Φ_{HL} structures ($c_{H^-}c_{HL}S_{HL,H^-}$). As shall be seen later, this sign change is associated with the effect that enables the BOVB wave function to confer efficient relaxation of the inactive electrons.

TABLE 4: Contribution to the Total TMH^+ Bond Discociation Energy from Ionic Configurations (ΔE_{mix})[a]

		VBSCF(3,full)				L-BOVB(3,full)			
		Φ_{H^+}		Φ_{H^-}		Φ_{H^+}		Φ_{H^-}	
entry		ΔE_{mix}	β	ΔE_{mix}	β	ΔE_{mix}	β	ΔE_{mix}	β
1	ScH^+	−4.3	−25.7	−1.1	−13.2	−6.3	−38.8	−18.0	160.1
2	TiH^+	−4.6	−27.7	−1.3	−14.9	−6.4	−40.8	−15.7	163.1
3	VH^+	−5.9	−30.6	−0.8	−11.9	−6.6	−40.2	−17.4	172.5
4	CrH^+	−6.4	−32.3	−1.1	−12.8	−8.0	−44.4	−25.2	205.0
5	MnH^+	−7.6	−33.8	−0.5	−10.0	−5.6	−41.6	−20.5	211.1
6	FeH^+	−8.7	−34.9	−0.4	−9.0	−10.1	−44.2	−28.5	247.9
7	CoH^+	−11.4	−39.2	−0.2	−6.7	−12.7	−47.8	−35.5	283.4
8	NiH^+	−12.8	−41.2	−0.1	−5.3	−14.8	−50.7	−42.0	313.5
9	CuH^+	−13.6	−43.8	−0.1	−4.4	−4.3	−54.8	−43.2	342.4
10	ZnH^+	−12.9	−42.9	−0.3	−7.9	*b*	*b*	*b*	*b*

[a] All values obtained from eq 8 with ST+f basis. Energies in kcal mol^{-1}. [b] The corrective addition of Φ_{HL}' renders the perturbation analysis of the ZnH^+ L-BOVB(4,full) results not meaningful.

SCHEME 4

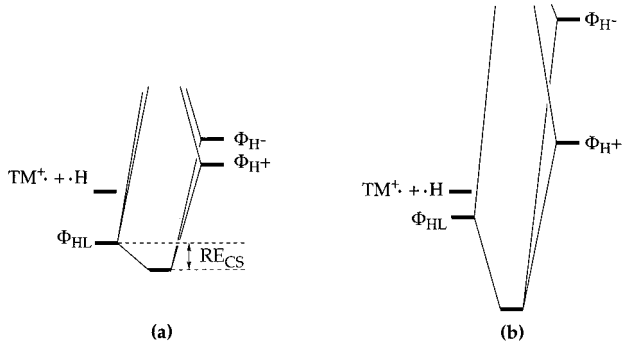

IV. Discussion

The significant improvement in BDEs (Table 2) upon moving from VBSCF(*n*,full) to L-BOVB(3,full) stands out among the results obtained in this study. To understand this feature we apply VB mixing ideas in the framework of perturbation theory to the three-structure wave function. Scheme 4 is a VB mixing diagram showing the mixing of the three VB configurations to form the bond state. At both VBSCF(3,full) (**4a**) and L-BOVB-(3,full) (**4b**) levels, the Φ_{H^+} and Φ_{H^-} structures are well above Φ_{HL}. The mixing energy of Φ_{H^+} and Φ_{H^-} into Φ_{HL} corresponds to the covalent-ionic resonance energy (RE_{CS}), which together with the self-stabilization of Φ_{HL} relative to the separate fragments comprises the total BDE at the given VB level. RE_{CS} can be further broken down into contributions from each ionic configuration, ΔE_{mix}, using the perturbation expression in eq 5 above.

The perturbation theory equations[76] (eqs 3−5 in the Methods section) reproduce the mixing energy and the mixing coefficients with qualitative and quite good quantitative accuracy and hence can be used in our qualitative analysis of these quantities. The results of the so calculated components of RE_{CS} along with the reduced resonance integral, β, are collected in Table 4. It is apparent that at the VBSCF level, the mixing of Φ_{H^+} is much more important than that of Φ_{H^-} . Furthermore, the energy contribution of the protio structure increases along the transition metal row, reaching ca. 13 kcal mol^{-1}. This trend is in accord with the expectation that, as a result of the imperfect screening by the 3d electrons along the TM series, the effective nuclear charge of TM^+ increases fast, and the vacant 4s orbital becomes increasingly a better electron acceptor. This in turn means that the $H \rightarrow TM^+$ charge transfer should increase as one proceeds from Sc^+ to Zn^+, as is indeed manifested by the variation of the H^+ charge in the series in Figure 3. It is apparent that *despite covalency of the bonds in VBSCF, a significant portion of the bonding energy comes from the mixing of the covalent HL and protio structures.* In contrast, the hydrido structure makes a small contribution to the stabilization of the bond pair and never exceeds ca. 1.1 kcal mol^{-1}.

At the L-BOVB level, the mixing coefficients (Table 3) are still larger for the protio configuration, and its energy contribution is about the same as in the VBSCF level. However, despite a small mixing coefficient, the energy contribution of the hydrido structure to the VB mixing is now significant and larger than the corresponding contribution due to the protio structure. This and the sign change in the mixing coefficient of the hydrido configuration can be understood by use of the perturbation theory equations (eq 3−5). Thus, eq 6 (based on eq 3) defines

$$\beta_{H^-} = (H_{HL,H^-}) - (e_{HL}S_{HL,H^-}) \tag{6}$$

the reduced resonance integral β_{H^-}, which is the effective matrix element responsible for the mixing[74,75] of the hydrido structure into the HL structure. The corresponding mixing coefficient is given by eq 7 (based on eq 4). Because the energy gap term in

$$\lambda_{H^-} = \beta_{H^-}/(e_{HL} - e_{H^-}) \tag{7}$$

eq 7 ($[e_{HL} - e_{H^-}]$) is always negative, the sign of the mixing coefficient will depend on the sign of the reduced resonance integral β_{H^-} . The values of this integral, which are collected in the last column in Table 4, are all positive and therefore lead to *negative mixing coefficients.* At the VBSCF(3,full) level, the reduced resonance integral is negative, and therefore the mixing coefficient is positive.

The energy contribution due to the mixing of the hydrido structure is given in turn by eq 8 (based on eq 5) as the product

$$\Delta E_{mix,H^-} = \lambda_{H^-}\beta_{H^-} \tag{8}$$

of the mixing coefficient and the reduced resonance integral.

As a result of the opposite sign of the two terms, the mixing energy contribution is always stabilizing (negative). Furthermore, the very large β_{H^-} values at the L-BOVB(3,full) level, as opposed to the small VBSCF(3,full) values, account also for the large L-BOVB(3,full) stabilization energy of the hydrido configuration, despite its small coefficient. Thus, perturbation theory accounts for the seemingly counterintuitive[49,51,77,78] change in the sign of the mixing coefficient of the hydrido structure at the BOVB level and the sharp increase in its energetic effect.

What is still needed is a clear physical explanation of the origins of the effect of the hydrido structure. The traditional effect of the VB mixing[74,75] between a HL structure and its

TABLE 5: Breakdown of the Bonding Contributions[a] for the TMH^+ Series[b]

						ΔE_{relax}(inactive)	
entry		D_{cov}[c]	ΔE_{Rumer}[c]	RE_{CS}[c]	ΔE_{relax}(bp)	$\Delta E_{relax}(3d^n)$	$\Delta E_{relax}(3s^23p^6)$
1	ScH^+	42.6	0.0	3.8	0.3	0.4	10.4
2	TiH^+	39.4	0.4	4.4	0.4	1.0	8.7
3	VH^+	36.4	0.7	4.5	0.4	2.1	9.0
4	CrH^+	3.1	1.5	4.9	1.1	4.1	11.4
5	MnH^+	22.8	2.8	5.0	0.2	3.7	9.5
6	FeH^+	28.6	2.1	5.3	0.2	6.8	10.9
7	CoH^+	19.6	1.8	5.8	1.3	7.8	12.5
8	NiH^+	8.5	1.5	6.1	1.4	11.3	11.5
9	CuH^+	−24.1	1.3	6.5	1.5	17.2	9.0
10	ZnH^+	39.0	0.0	7.2	0.6	$\Delta E_{relax}(3d^{10}3s^23p^6) = 8.9$[d]	

[a] Equation 9. [b] All values in kcal mol^{-1} obtained with ST+f basis. [c] These terms sum up to the VBSCF(*n*,full) bond energy in Table 2. [d] Calculated with four VB states as described in the text. Dissection to the $3d^{10}$ and $3s^23p^6$ terms for the four-structure calculation is not meaningful.

charge-shifted structures (such as the hydrido structure) is to increase bonding relative to the covalent situation by delocalizing the bond-pair electrons over the two atomic centers that participate in the bond. According to the rules of qualitative VB theory,[74,75] the reduced resonance integral that characterizes such a VB interaction *is negative* and signed like the direct matrix element (H_{HL,H^-} in eq 6) between the orbitals that participate in the electron shift between the VB structures. These rules assume, of course, that the active and inactive orbitals are exactly the same for all of the VB structures, which is a correct assumption at the VBSCF level. Thus, VBSCF obeys the rules of qualitative VB theory, and the VB structures fulfill their roles of delocalizing the bond-pair electrons over the two atomic centers.

During the BOVB procedure, additional stabilization is attained by allowing all of the orbitals to change from one structure to the other. Thus, occasionally the VB structures of the highest energy, in addition to their traditional role, will assume the major role of relaxing the inactive electron pairs. The mixing of Φ_{HL} and Φ_{H^+} structures is important for delocalizing the bond pair and optimizing thereby the bonding between the TM and the hydrogen, and therefore the orbitals of these structures retain their essential VB characters; their reduced resonance integral remains negative as required by the rules of qualitative VB theory. On the other hand, the Φ_{H^-} configuration is less important for optimizing the bond at the VBSCF level, and this feature does not change in BOVB. However, because the contribution of Φ_{H^-} to the wave function is small, it is of no significant consequence to the total energy if the orbitals of this structure would change significantly to cater for the relaxation of the inactive electrons. Indeed, the hydrido structure rises steeply in energy during the BOVB procedure, and its inactive orbitals change much more than those of Φ_{H^+}.[79] The mixing of Φ_{H^-} with Φ_{HL} is dominated by the changes in the inactive orbitals. This change in the nature of the mixing is manifested in the sign change of the reduced matrix element, β_{H^-}, to a positive quantity. *As such, the Φ_{H^-} configuration does not merely represent the $TM^{2+}H^-$ structure in its VB sense but also serves as a degree of freedom by which the wave function relaxes the inactive electrons and improves its response to the fluctuation of charge inherent in the VB mixing of the principal structures Φ_{HL} and Φ_{H^+}.*

VB theory enables the testing of the foregoing analysis by performing the BOVB(3) computation in the stepwise manner depicted in Scheme 5. Thus, the BOVB procedure starts by enabling only the bond-pair (bp) electrons to breathe, while freezing all of the inactive electrons as obtained at the VBSCF-(3,full) level, resulting in the BOVB(3,bp) level. The resulting energy increment provides the relaxation energy of the bond

SCHEME 5

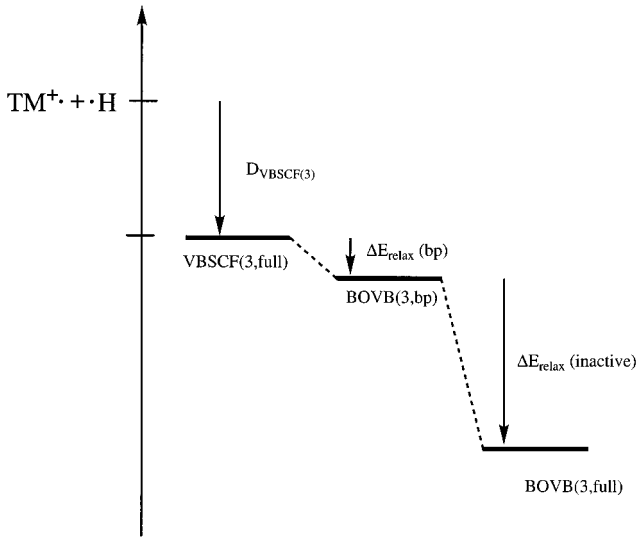

pair electrons, ΔE_{relax}(bp). Subsequently, the inactive orbitals are allowed to breathe, and the corresponding energy change constitutes the relaxation energy of the inactive electrons, ΔE_{relax}-(inactive). Table 5 shows these energy increments for the TMH^+ series, and it is apparent that all of the ΔE_{relax}(bp) terms are extremely small. Thus, the effect of the hydrido configuration on the bond-pair electrons remains small at the L-BOVB(3,bp) level, and the corresponding bond energy hardly exceeds the VBSCF value. On the other hand, the ΔE_{relax}(inactive) terms (columns 7 and 8, Table 5) are significant and constitute the major effect at the L-BOVB(3,full) level. It follows that the Φ_{H^-} configuration, in addition to its small contribution to the bond pairing, serves primarily to relax and correlate the inactive 3s and 3p core and 3d electrons, relative to the bond electrons.[80]

Contributions to the TM−H^+ Bond Energy. Understanding the role of the hydrido structure provides the means to analyze the bonding origins in terms of VB concepts such as covalency and ionicity, as well as the relaxation of the inactive "environment" in response to the fluctuation of the charge density in the bond. This is done by appeal to eq 9 where D_{TMH^+}

$$D_{TMH^+}[\text{L-BOVB(3,full)}] = D_{cov} + \Delta E_{Rumer} + RE_{CS} + \Delta E_{relax}(bp) + \Delta E_{relax}(3d^n) + \Delta E_{relax}(3s^2p^6) \quad (9)$$

corresponds to BDE. Here, D_{cov} refers to the covalent bond energy due to the principal HL structure (itself variationally optimized), and ΔE_{Rumer} accounts for the other covalent electron coupling schemes. The RE_{CS} term refers to the charge-shift

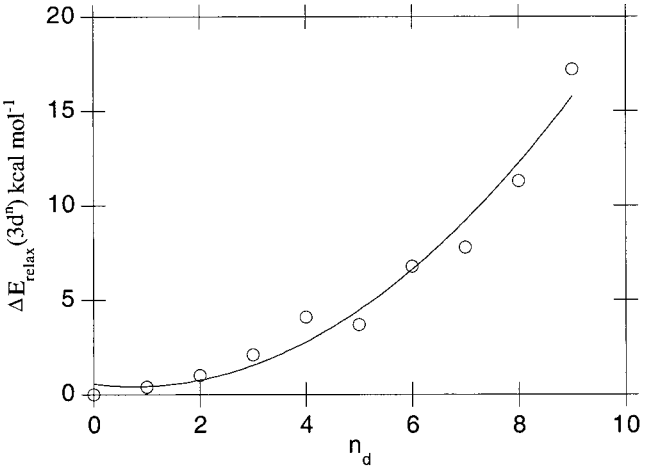

Figure 4. The effect of electron correlation due to 3d electrons in TMH^+. $\Delta E_{relax}(3d^n)$ is the energetic difference between allowing only active orbitals to breathe and allowing active and 3d orbitals to breathe. In each case all other orbitals are taken from the corresponding VBSCF-(3,full) calculation and held frozen. ZnH^+ is not included in the plot because of the negligible effect of the completely full d shell (see text).

resonance energy due to the traditional delocalization of the bond-pair electrons via the mixing of the ionic structures' Φ_{H^+} and Φ_{H^-} into the Φ_{HL} structure. $\Delta E_{relax}(bp)$ accounts for the relaxation energy of the bond-pair electrons when the bond orbitals are allowed to breathe. *These four terms give the optimal contribution to bonding due to the spin pairing of the bond-pair electrons.*

The last two terms account for the relaxation energy of the inactive electrons that are not involved in bonding. These are the electrons in the $3s^23p^63d^n$ subshell, which is further broken down into $3s^23p^6$ and $3d^n$ groups. The corresponding ΔE terms quantify therefore *the response of the nonbonding and adjacent core electrons to the charge fluctuation of the bond pair* (Scheme 5).

The ΔE quantities are collected in Table 5, which reveals traditional as well as novel trends. The bonding contribution due to the bond-pair electrons (first four energy columns) is dominated in most cases by D_{cov}, as expected from the dominant covalent nature of the bond. The RE_{CS} contribution increases from the left to the right of the TMH^+ series, following the expected increase of the Φ_{HL}/Φ_{H^+} mixing due to the increasing electron affinity of the transition metal cation (TM^+). Note though, that despite the dominance of D_{cov}, *the RE_{CS} term is never negligible, and in some cases it is even close to or greater than D_{cov}*, for example, in CrH^+ and NiH^+. Thus, although TM−H^+ bonds are not charge-shift (CS) bonds, their apparent covalency conceals the important CS contribution.

The novel trend in Table 5 belongs to the behavior of the ΔE_{relax}(inactive) terms. The $\Delta E_{relax}(3d^n)$ term is seen to increase as the number of nonbonding 3d electrons increases from ScH^+ to CuH^+. Indeed, a plot of $\Delta E_{relax}(3d^n)$ against the number of d electrons (n_d) in Figure 4 shows a direct correlation, which is expressed in eq 10. The small intercept (~0.5 kcal mol^{-1}) is

$$\Delta E_{relax}(3d^n)\ \text{kcal mol}^{-1} = 0.56 - 0.35n_d + 0.23n_d^2 \qquad (10)$$

an indication that the correlation is physically correct. In line with this reasoning, the $\Delta E_{relax}(3s^23p^6)$ term is roughly constant, 10.6 ± 1.9 kcal mol^{-1}, presumably because it accounts for a constant number of electrons.

Inspection of the ΔE_{relax}(inactive) term, shows that this term contributes ca. 16−60% of the total bond energy. It is somewhat less important for the early TMH^+ species ScH^+, TiH^+, and VH^+, as well as for ZnH^+, but it makes an important contribution for all of the late TMH^+ species, starting from CrH^+ onward to CuH^+. In CuH^+, the bond-pairing energy is negative (−14.8 kcal mol^{-1}) as a result of the high cost of the $3d^{n+1} \rightarrow 3d^n4s^1$ promotion needed to prepare Cu^+ for bonding with H. *Clearly, electron-pairing in such cases provides the means for inactive electrons to relax and lower their Pauli repulsion. It is clear that as a result of the frequent weakness of transition metal bonds ($D < 60$ kcal mol^{-1}), we may expect that the relaxation response energy of the nonbonding and core sub shells will generally be an important factor in transition metal compounds.*

Do we have to worry about all of the core electrons? The example of ZnH^+ (entry 10, Table 5) indicates that the answer is negative. Thus, as shown by Goddard and co-workers,[11] in $Zn-H^+$ the bond pair is mainly Zn(4s)−H(1s) with little Zn-($3d_\sigma$) contribution. Apparently, the $3d^{10}3s^23p^6$ subshell of Zn^+ is contracted and behaves as an inner shell that contributes ca. 16% of the total bond energy. This suggests in turn that core electrons beyond the subvalence shell are not likely to make very important contributions to bonding.

V. Conclusions

The VBSCF method reproduces trends in the experimental bond dissociation energies of the transition metal hydride cations ScH^+ to ZnH^+. The more flexible L-BOVB method is required for a more quantitative agreement with experiment comparable to CCSD(T) results. This shows that modern valence bond methods are useful for studies involving transition metals.

The calculations show that despite the very covalent nature of the bonds (≥90% in terms of weight), the bond energy is augmented by two other contributions. One is the charge shift resonance energy due to the mixing of the ionic structures (Φ_{H^+}, Φ_{H^-}) into the covalent structure (Φ_{HL}). The second and larger contribution is the relaxation energy of the nonbonding $3d^n$ electrons and the adjacent core electrons ($3s^23p^6$). The relaxation makes a major contribution to bonding for late TMH^+ molecules. Thus, it appears that in these covalent bonds the electron pairing of the "bonding electrons" is a trigger that enables all of the nonbonding and adjacent core electrons to relax their Pauli repulsions and provide the molecule with a significant stability. Because $TM-H^+$ bonds are inherently weak, the relaxation response of the inactive and adjacent core electrons would be expected to constitute a major bonding event. One wonders, therefore, how many more covalent bonds are of the same flavor.

Acknowledgment. This work was supported by the Volkswagenstiftung (VW) and the Israel Science Foundation (ISF) established by the Israel Academy of Sciences and Humanities. J.M.G. is partially supported by the Lady Davis Fellowship Trust at the Hebrew University. The authors would like to thank Prof. Philippe Hiberty for helpful suggestions during his visit to the Lise-Meitner Minerva Center regarding how to overcome the BOVB overbinding and Dr. Nathan Harris for helpful proofing of this manuscript.

Supporting Information Available: A table of total energies. This material is available free of charge via the Internet at http://pubs.acs.org.

References and Notes

(1) Martinho Simoes, J. A.; Beauchamp, J. L. *Chem. Rev.* **1990**, *90*, 629.

(2) Meunier, B. *Chem. Rev.* **1992**, *92*, 1411.

(3) Wing, R. F.; Cohen, J.; Brault, J. W. *J. Chem. Phys.* **1983**, *78*, 2097.
(4) Crabtree, R. H. *Angew. Chem., Int. Ed. Eng.* **1993**, *32*, 789.
(5) Eller, K.; Schwarz, H. *Chem. Rev.* **1991**, *91*, 1121.
(6) *Polyhedron* **1988**, *16/17*, entire issue dedicated to organometalic TM complexes.
(7) Allison, J. *Prog. Inorg. Chem.* **1986**, *34*, 627.
(8) Pearson, R. G. *Chem. Rev.* **1985**, *85*, 41.
(9) Allison, J. *Acc. Chem. Res.* **1982**, *15*, 238.
(10) Ohanessian, G.; Goddard, W. A. *Acc. Chem. Res.*, **1990**, *23*, 386.
(11) Schilling, J. B.; Goddard, W. A.; Beauchamp, J. L. *J. Phys. Chem.* **1987**, *91*, 5616.
(12) Schilling, J. B.; Goddard, W. A.; Beauchamp, J. L. *J. Am. Chem. Soc.* **1987**, *109*, 5565.
(13) Schilling, J. B.; Goddard, W. A.; Beauchamp, J. L. *J. Am. Chem. Soc.* **1986**, *108*, 582.
(14) Petterson, L. G. M.; Bauschlicher, C. W.; Langhoff, S. R.; Partridge, H. *J. Chem. Phys.* **1987**, *87*, 481.
(15) Ziegler, T.; Li, J. *Can. J. Chem.* **1994**, *72*, 783.
(16) Barone, V.; Adamo, C. *Int. J. Quantum Chem.* **1997**, *61*, 443.
(17) Areste, N.; Armentrout, P. B. *J. Am. Chem. Soc.* **1984**, *106*, 4065.
(18) Elkind, J. L.; Armentrout, P. B. *Inorg. Chem.* **1986**, *25*, 1078.
(19) Armentrout, P. B.; Beauchamp, J. L. *Acc. Chem. Res.* **1989**, *22*, 315.
(20) Carter, E. A.; Goddard, W. A. *J. Phys. Chem.* **1988**, *92*, 2109.
(21) Walch, S. P.; Bauschlicher, C. W. *J. Chem. Phys.* **1983**, *78*, 4597.
(22) Walch, S. P.; Goddard, W. A. *J. Am. Chem. Soc.* **1976**, *100*, 1338.
(23) Carlson, K. D.; Moser, C. *J. Chem. Phys.* **1966**, *44*, 3259.
(24) Carlson, K. D.; Ludena, E.; Moser, C. *J. Chem. Phys.* **1965**, *43*, 2408.
(25) Carlson, K. D.; Nesbet, R. K. *J. Chem. Phys.* **1964**, *41*, 1051.
(26) Bauschlicher, C. W.; Langhoff, S. R.; Partridge, H.; Barnes, L. A. *J. Chem. Phys.* **1989**, *91*, 2399.
(27) Armentrout, P. B.; Georgadis, R. *Polyhedron* **1988**, *7*, 1573.
(28) Barnes, L. A.; Rosi, M.; Bauschlicher, C. W. *J. Chem. Phys.* **1990**, *93*, 609.
(29) Mavridis, A.; Harrison, J. F.; Allison, J. *J. Am. Chem. Soc.* **1989**, *111*, 2482.
(30) Allison, J.; Mavridis, A.; Harrison, J. F. *Polyhedron*, **1988**, *7*, 1559.
(31) Bauschlicher, C. W.; Barnes, L. A. *Chem. Phys.* **1988**, *124*, 383.
(32) Loades, S. D.; Cooper, D. L.; Gerratt, J.; Raimondi, M. *J. Chem. Soc., Chem. Commun.* **1989**, 1604.
(33) (a) Verbeek, J.; Langenberg, J. H.; Byrman, C. P.; Van Lenthe, J. H. *TURTLE*, ab initio VB/VBSCF/VBCI program; Theoretical Chemistry Group, Debye Institute, University of Utrecht, 1993. (b) van Lenthe, J. H.; Balint Kurti, G. G. *Chem. Phys. Lett.* **1980**, *76*, 138. van Lenthe, J. H.; Balint Kurti, G. G. *J. Chem. Phys.* **1983**, *78*, 5699.
(34) Hiberty, P. C. In *Modern Electronic Structure Theory and Applications in Organic Chemistry*; Davidson, E. R., Ed.; World Scientific: River Edge, NJ, 1997; pp 289−367.
(35) Hiberty, P. C. *J. Mol. Struct. (THEOCHEM)* **1998**, *451*, 237.
(36) Hiberty, P. C.; Flament, J. P.; Noizet, E. *Chem. Phys. Lett.* **1992**, *189*, 259.
(37) Hiberty, P. C.; Humbel, S.; Byrman, C. P.; Van Lenthe, J. H. *J. Chem. Phys.* **1994**, *101*, 5969.
(38) Bobrowicz, F. W., Goddard, W. A. *Modern Theoretical Chemistry: Methods of Electronic Structure Theory;* Schaefer, H. F., Ed.; Plenum: New York, 1977; Vol. 3, p 79.
(39) Lewis, G. N. *J. Am. Chem. Soc.* **1916**, *38*, 762.
(40) Langmuir, I. *J. Am. Chem. Soc.* **1919**, *41*, 868 and 1543.
(41) Pauling, L. *The Nature of the Chemical Bond*, 2nd ed.; Cornell University Press: Ithaca, NY, 1940.
(42) Heitler, W.; London, H. F. *Z. Physik* **1927**, *44*, 455.
(43) A simple transformation of the GVB wave function, e.g., for H_2, leads to a mixture of HL and ionic structures. More on this equivalency can be found in Hiberty, P. C.; Cooper, D. L. *J. Mol. Struct. (THEOCHEM)* **1988**, *169*, 437 and ref 34.
(44) Coulson, C. A.; Fischer, I. *Philos. Mag.* **1949**, *40*, 386.
(45) Hiberty, P. C.; Humbel, S.; Archirel, P. *J. Phys. Chem.* **1994**, *98*, 11697.
(46) Lauvergnat, D.; Maître, P.; Hiberty, P. C.; Volatron, F. *J. Phys. Chem.* **1996**, *100*, 6463.
(47) Shaik, S. S.; Maître, P.; Sini, G.; Hiberty, P. C. *J. Am. Chem. Soc.* **1992**, *114*, 7861.
(48) Sini, S.; Maître, P.; Hiberty, P. C.; Shaik, S. S. *J. Mol. Struct. (THEOCHEM)* **1991**, *229*, 163.
(49) Shurki, A.; Hiberty, P. C.; Shaik, S. *J. Am. Chem. Soc.* **1999**, *121*, 822.
(50) Lauvergnat, D.; Hiberty, P. C.; Danovich, D.; Shaik, S. *J. Phys. Chem.* **1996**, *100*, 5715.
(51) Danovich, D.; Wu, W.; Shaik, S. *J. Am. Chem. Soc.* **1999**, *121*, 3165.
(52) Hay, P. J.; Wadt, W. R. *J. Chem. Phys.* **1985**, *82*, 270.
(53) Dunning, T. H., Jr.; Hay, P. J. In *Methods of Electronic Structure Theory;* Schaefer, H. F., III, Ed.; Plenum Press: New York, 1977; Vol. 2.
(54) Dolg, M.; Wedig, U.; Stoll, H.; Preuss, H. *J. Chem. Phys.* **1987**, *86*, 866.
(55) Dunning, T. H., Jr. *J. Chem. Phys.* **1971**, *55*, 716.
(56) Wachters, A. J. H. *J. Chem. Phys.* **1970**, *52*, 1033.
(57) Hay−Wadt+f from 6-311G**, Hay, P. J. *J. Chem. Phys.* **1977**, *66*, 4377. ST+f from ref 3. Wachters+f from Bauschlicher, C. W., Jr.; Langhoff, S. R.; Barnes, L. A. *J. Chem. Phys.* **1977**, *66*, 4377.
(58) The Hay−Wadt, Wachters+f, and Dunning basis sets were obtained from the Extensible Computational Chemistry Evironment Basis Set Database, Version 1.0, as developed and distributed by the Molecular Science Computing Facility, Environmental and Molecular Sciences Laboratory, which is part of the Pacific Northwest Laboratory, P.O. Box 999, Richland, WA 99352 and is funded by the U.S. Department of Energy. The Pacific Northwest Laboratory is a multiprogram laboratory operated by Battelle Memorial Institute for the U.S. Department of Energy under contract DE-AC06-76RLO 1830. Contact David Feller, Karen Schuchardt, or Don Jones for further information; http://www.emsl.pnl.gov: 2080/forms/basisform.htm/.
(59) Bartlett, R. J.; Purvis, G. D. *Int. J. Quantum Chem.* **1978**, *14*, 167.
(60) For CCSD(T) implementation in GAUSSIAN, see Pople, J. A.; Head-Gordon, M.; Raghavachari, K. *J. Chem. Phys.*, **1987**, *87*, 5968.
(61) Frisch, M. J.; Trucks, G. W.; Schlegel, H. B.; Gill, P. M. W.; Johnson, B. G.; Robb, M. A.; Cheeseman, J. R.; Keith, T.; Petersson, G. A.; Montgomery, J. A.; Raghavachari, K.; Al-Laham, M. A.; Zakrzewski, V. G.; Ortiz, J. V.; Foresman, J. B.; Cioslowski, J.; Stefanov, B. B.; Nanayakkara, A.; Challacombe, M.; Peng, C. Y.; Ayala, P. Y.; Chen, W.; Wong, M. W.; Andres, J. L.; Replogle, E. S.; Gomperts, R.; Martin, R. L.; Fox, D. J.; Binkley, J. S.; Defrees, D. J.; Baker, J.; Stewart, J. P.; Head-Gordon, M.; Gonzalez, C.; Pople, J. A. *Gaussian 94*, revision D.4; Gaussian, Inc.: Pittsburgh, PA, 1995.
(62) Banerjee, A.; Grein, F. *Int. J. Quantum Chem.* **1976**, *10*, 123.
(63) Grein, F.; Chang, T. C. *Chem. Phys. Lett.* **1971**, *12*, 44.
(64) Levy, B.; Berthier, G. *Int. J. Quantum Chem.* **1968**, *2*, 307.
(65) Gerratt, J.; Cooper, D. L.; Karadakov, P. B.; Raimondi, M. *Chem. Soc. Rev.* **1997**, 87. Cooper, D. L.; Gerratt, J.; Raimondi, M. *Chem. Rev.* **1991**, *91*, 927.
(66) For a recent SCVB treatment of $TMCH_2^+$ (TM = Sc, Ti), see Ogliaro, F.; Cooper, D. L.; Kardakov, P. B. *Int. J. Quantum Chem.* **1999**, *74*, 223. We thank F. Ogliaro for communicating the paper.
(67) Langhoff, S. R.; Bauschlicher, C. W.; Partridge, H. In *Comparison of ab Initio Quantum Chemistry with Experiment for Small Molecules*; Bartlett, R. J., Ed.; Reidel: Dordrecht, 1985.
(68) Moore, C. E. *Atomic Energy Levels*; National Bureau of Standards: Washington, DC, 1971; Vols. I and II.
(69) Pauncz, R. *Spin Eigenfunctions*; Plenum Press: London, 1979; p 21.
(70) The bond pair in, e.g., **3a**, is actually a hybrid of 4s and $3d_\sigma$. However, the 4s contribution to the bond hybrid is always dominant.
(71) Hiberty, P. C.; Byrman, C. P. *J. Am. Chem. Soc.* **1995**, *117*, 9875.
(72) A wave function with split orbitals is precisely transformed to a wave function that involves double excitation.
(73) Chirgwin, H. B.; Coulson, C. A. *Proc. R. Soc. London, Ser. A* **1950**, *2*, 196.
(74) Shaik, S. S. In *New Concepts for Understanding Organic Reactions*; Betrán, J., Csizmadia, I. G., Eds.; Kluwer Academic Publishers: Norwell, MA, 1989; Vol C267.
(75) Shaik, S.; Hiberty, P. C. *Adv. Quantum Chem.* **1995**, *26*, 99.
(76) Libit, L.; Hoffmann, R. *J. Am. Chem. Soc.* **1974**, *96*, 1370.
(77) Ammeter, J. H.; Burgi, H.-B.; Thibeault, J. C.; Hoffmann, R. *J. Am. Chem. Soc.*, **1978**, *100*, 3686.
(78) Whangbo, M.-H.; Hoffmann, R. *J. Chem. Phys.* **1978**, *68*, 5498.
(79) Using ScH^+ as a representative example, the energy of the Φ_{H^-} structure goes from 162 kcal mol^{-1} to 1424 kcal mol^{-1} above the separated fragments upon moving from VBSCF(3,full) to L-BOVB(3,full). A plot of the L-BOVB(3,full) orbitals shows the inactive 3p orbitals centered on Sc in the Φ_{H^-} structure to be more polarized away from the hydrogen relative to the corresponding orbitals of the Φ_{HL} structure, while VBSCF(3,full) orbitals are seen to be nearly identical with those of the L-BOVB(3,full) Φ_{HL} structure. All orbital plots were done using *MOLDEN*; Schaftenaar, G. CAOS/CAMM Center: The Netherlands, http://www-srs.caos.kun.nl/~schaft/molden/molden.html
(80) This was tested also by performing BOVB(2,full) using Φ_{HL} and Φ_{H^+} only. The resulting energy was short of the final bond energy by approximately ΔE_{relax}(inactive). Thus, even though all of the inactive orbitals were allowed to optimize, the 2×2BOVB did not produce the relaxation effect. Adding Φ_{H^-} with frozen orbitals taken from the VBSCF calculation had no effect on the bond energy, in line with its unimportance for bond pairing. Only when the Φ_{H^-} orbitals were allowed to optimize did they undergo a significant change[79] and provide a large improvement to the bond energy, in line with the assigned role of Φ_{H^-} as a means to relax the inactive electrons in response to the bond pairing.